AMPylation of Rho GTPases by *Vibrio* VopS disrupts effector binding and downstream signaling

We have discovered that the *Vibrio parahaemolyticus* effector VopS is an AMPylator that uses ATP to modify Rho GTPases with adenosine 5'-monophosphate, thereby preventing interaction with downstream effectors that mediate actin assembly. We demonstrate that eukaryotic proteins can modify proteins with AMP and propose that this previously undescribed modification presents a new paradigm for molecular signaling.

Melanie L. Yarbrough[1], Yan Li[2,3], Lisa N. Kinch[4], Haydn L. Ball[2,3] & Kim Orth[1*]

[1] Department of Molecular Biology

[2]Protein Chemistry Technology Center

[3]Department of Internal Medicine

[4] Department of Biochemistry

UT Southwestern Medical Center

Dallas, TX 75390

*To whom correspondence should be addressed:

UTSWMC 5323 Harry Hines Blvd., Dallas, TX 75390-9148

Ph 214-648-1685 Fax 214-648-1488 Kim.Orth@utsouthwestern.edu

Abstract

The *Vibrio parahaemolyticus* type III effector VopS is implicated in cell rounding and the collapse of the actin cytoskeleton by inhibiting Rho GTPases. We show VopS is an AMPylator that covalently modifies a conserved threonine residue on Rho, Rac and Cdc42 with adenosine 5'-monophosphate. The resulting AMPylation prevents interaction of Rho GTPases with downstream effectors, thereby inhibiting actin assembly in the infected cell. We demonstrate that eukaryotic proteins are modified with AMP and propose that this previously undescribed eukaryotic modification presents a new paradigm for molecular signaling.

Vibrio parahaemolyticus (*V. parahaemolyticus*) is a Gram-negative, halophilic bacterium that is a major cause of food-borne illness worldwide, and infections lead to acute gastroenteritis (*1*). In Southeast Asia, it is the most common source of infection from consumption of undercooked and raw seafood, particularly shellfish (*2*). Pandemic strains are emerging throughout the world and recent studies implicate climate changes due to global warming in triggering the spread of *V. parahaemolyticus* as far north as the coastal waters of Alaska (*3*).

Sequencing of a pathogenic strain of *V. parahaemolyticus* revealed the presence of a previously well-characterized virulence factor called the thermostable direct hemolysin (TDH) and two type III secretion systems (T3SS), one located on chromosome one (T3SS1) and the second located on a pathogenicity island of chromosome two (T3SS2) (*4*). These bacterial T3SSs deliver proteins, called effectors, into the cytosol of host cells during infection (*5*). T3SS2 is found only in clinical isolates of *V. parahaemolyticus* and is associated with enterotoxicity in a rabbit ileal loop model (*6*). Recently, we demonstrated that T3SS1 uses a multifaceted mechanism to cause cytotoxicity of host cells, involving induction of autophagy, cell rounding and cell lysis (*7*). These events appear to occur in parallel and support the hypothesis that multiple effectors induce cytotoxicity.

One of the effectors secreted by T3SS1, VopS (VP1686), has been implicated in cell rounding by inactivation of Rho family GTPases, including Rac, Rho and Cdc42 (*8*). After one hour of infection with the *V. parahaemolyticus* POR3 strain, which contains a functional T3SS1 and inactivating mutations for both TDHs and T3SS2, we observed the presence of active GTP-bound Cdc42 as measured by the ability of Cdc42 to interact with a GST fusion of its downstream effector, the Cdc42 binding domain of p21-activated kinase 3 (GST-PAK PBD) (Fig. 1A, lane 2) (*7, 9*). Beyond one hour post infection, the presence of VopS in the POR3 strain is consistent with inactivation of Cdc42, as the population of active GTP-bound Cdc42 is no longer observed in infected cells (Fig. 1A, lanes 3-5). When infected with a POR3 strain containing a deletion of VopS (POR3Δ*vopS*), levels of Cdc42 in the active GTP-bound state persist, but all Cdc42 is eventually inactivated by 4 hours (Fig. 1A, lanes 6-9). Reconstitution of the deletion strain with a wild-type copy of VopS caused a loss of active Cdc42 one hour after

infection, similar to the POR3 strain (Fig. 1A, lanes 10-13). In studies with all three strains, the total level of Cdc42 is reduced at the later time points of infection. Based on these observations, we propose that VopS inactivates the Rho family GTPases early in infection, while another factor exists that may contribute to the destabilization of Rho family GTPases later in infection. Further support of this hypothesis comes from the observation that although cell rounding is delayed with the POR3Δ*vopS* strain, it eventually occurs at approximately 3 hours post infection (Fig. S1A).

Expression of full-length VopS is sufficient to induce a severely rounded phenotype in transfected HeLa cells, supporting the previous observation that a VopS-dependent disruption of Rho GTPase signaling occurs during infection (Fig. 1B) (8). VopS includes a C-terminal domain of unknown function called Fic (filamentation induced by cAMP). Fic domain sequences are found in a variety of species and contain an invariant histidine (H) within a conserved motif (HPFx(D/E)GNGR) (*11*) (Fig. 1C). Mutation of the Fic domain at this conserved histidine (VopS-H348A) abrogates the VopS-mediated cell rounding (Fig. 1B). Since VopS is an effector secreted by T3SS1 during infection, we next determined whether the secretion signal sequence of VopS is required for its cell rounding activity. We created an amino-terminal truncation of VopS (VopSΔ30) that deletes the putative signal sequence and observed that this mutant induces rounding of transfected HeLa cells in a fashion similar to that observed for wild-type VopS (Fig. 1B). As expected, VopSΔ30-H348A does not cause any obvious changes in the actin cytosketon of transfected cells (Fig. 1B). Thus far, we have established that VopS contributes to the rounding phenotype observed in infected cells by a mechanism that requires a wild-type Fic domain but is independent of its signal sequence.

We next performed a series of *in vitro* experiments to elucidate the biochemical mechanism used by VopS to inhibit Rho family of GTPases. To aid in the purification of recombinant VopS, we used the active VopSΔ30 that lacks the largely hydrophobic 30 amino acid signal sequence. Using pulldown assays, we observed that although ^{35}S-radiolabeled Rac does not interact with GST-VopSΔ30 (Fig. 2A, lane 4), it does interact with GST-VopSΔ30-H348A (Fig. 2A, lane 5). In addition, GTP loading of the ^{35}S-radiolabeled Rac increases the amount of ^{35}S-radiolabeled Rac that can interact with recombinant VopSΔ30-H348A (Fig. 2A, compare lanes 5 and 9). This result is

reminiscent of the conformation-dependent interaction of GTP-bound Rac with its downstream effector PAK (*12*). When we load ^{35}S-radiolabeled Rac with GTP, we observe that more ^{35}S-radiolabeled Rac interacts with GST-PAK PBD (Fig. 2A, compare lanes 3 and 7). Many type III effectors use a catalytic mechanism to alter eukaryotic signaling pathways, and in some cases the catalytically inactive form of the effector can act as a substrate trap (*13*). Based on our binding experiments, we speculate that VopSΔ30-H348A mutant might act as a trap by binding its substrate, the active GTP-bound Rac, but failing to release a product.

To further analyze the possibility that GTP-bound Rho family GTPases might be substrates for VopS, we produced the ^{35}S-radiolabeled dominant active form of Rac (DA-Rac) that is unable to hydrolyze GTP and thus remains constitutively active. We pre-incubated ^{35}S-radiolabeled DA-Rac with 25 pmoles of purified recombinant VopSΔ30 or VopSΔ30-H348A and then tested whether the ^{35}S-radiolabeled DA-Rac is able to interact with its downstream effector, GST-PAK PBD. While ^{35}S-radiolabeled DA-Rac pre-incubated with the mutant VopSΔ30-H348A interacts with GST-PAK PBD, ^{35}S-radiolabeled Rac pre-incubated with VopSΔ30 is unable to interact with GST-PAK PBD (Fig. 2B). We then pre-incubated ^{35}S-radiolabeled DA-Rac with serial 10-fold dilutions of purified recombinant VopSΔ30 (125-0.125 pmoles) for 15 minutes and tested whether the ^{35}S-radiolabeled DA-Rac could bind to GST-PAK PBD (Fig. 2C). Incubation of ^{35}S-radiolabeled DA-Rac with as little as 1.25 pmoles of VopSΔ30 prevents the binding of ^{35}S-radiolabeled DA-Rac to GST-PAK PBD (Fig. 2C, lane 6). As expected, incubation of DA-Rac with decreasing amounts of VopSΔ30-H348A has no effect on the ability of DA-Rac to bind to GST-PAK PBD (Fig. 2C, lanes 8-11). Next, we incubated ^{35}S-radiolabeled DA-Rac with a limiting amount of VopSΔ30 (0.25 pmoles) over a time course of one hour, and observed that by 40 minutes no ^{35}S-radiolabeled DA-Rac interacts with GST-PAK PBD (Fig. 2D, lane 6). Based on the concentration and time dependence of the inhibitory effect, we hypothesize that VopS uses an enzymatic activity to inhibit the interaction of Rho family GTPases with their respective downstream effectors.

To determine the activity that VopS exerts on the Rho family GTPases, we expressed His-tagged DA-Rac either alone (DA-Rac) or with active GST-tagged

VopSΔ30 (DA-Rac/VopS). Both forms of recombinant DA-Rac can be loaded with ^{35}S-radiolabeled GTPγS, a non-hydrolyzable form of GTP, eliminating the possibility that VopS inhibits the Rho family of proteins by preventing GTP binding (Fig. 3A). To determine if DA-Rac is altered by coexpression with VopS, we measured the mass of recombinant DA-Rac by mass spectrometry. While DA-Rac expressed alone had the expected molecular weight, DA-Rac/VopS had an increase in molecular weight of 329 daltons (Fig. S2, A and B). As expected, DA-Rac coexpressed with the mutant VopS did not show an increase in molecular weight (data not shown). The increase of 329 daltons is consistent with the mass of adenosine 5'-monophosphate (AMP). To identify where this putative covalent modification occurs on Rac, we analyzed tryptic and AspN peptides using liquid chromatography followed by mass spectrometry. When the samples were digested with AspN, peptide A [aa 11-37, mass-to-charge ratio (m/z) of 1488.7 when z = 2] is observed for DA-Rac (Fig. 3B). For DA-Rac/VopS, only the modified form of peptide A is observed [aa 11-37, with a mass increase of 329.1 Da, m/z = 1653.3 when z = 2] (Fig. 3C). Further analysis of peptide A from DA-Rac/VopS using LC-MS/MS revealed that the peptide contains a covalent modification of 329 daltons on Thr35, a conserved residue located in the effector loop of the switch I region of Rho family GTPases (Fig. 3D) (*12*). This region of the Rho GTPases is highly conserved and plays a role in GTP, Mg^{2+} and effector binding (Fig. 3E) (*12, 14*). Based on these results, we postulate that VopS modifies the Rho family GTPases with AMP, which thereby prevents Rho GTPases from binding to downstream effectors by steric hindrance.

To test directly whether VopS functions as an enzyme to modify Rho family GTPases with AMP, we performed an *in vitro* labeling assay with ^{32}P-α-labeled ATP, VopS and Rho family GTPases. After incubation of purified recombinant VopSΔ30 with or without purified recombinant DA-Rac, and ^{32}P-α-labeled ATP, we observed that DA-Rac is modified in a VopS-dependent manner (Fig. 4A, lane 2). To confirm that the modification is specific for the predicted Thr35 on the switch I region of Rac, we mutated Thr35 to alanine (DA-Rac-T35A). VopSΔ30 does not modify a DA-Rac-T35A mutant, supporting our previous observations that the AMP modification is specific for Thr35 (Fig. 4A, lane 3). As expected, we observed no modification of DA-Rac incubated with VopS-H348A (Fig. 4A, lanes 4-6). To confirm that VopS modifies other members of the

Rho family GTPases, we repeated the *in vitro* labeling assay using Rho, Rac, and Cdc42. In the presence of VopS, all of the GTPases are modified by AMP, whereas they are not modified in the presence of only ^{32}P-α-labeled ATP or by VopS-H348A (Fig. 4B). Therefore, we conclude that VopS modifies Rho GTPases with AMP. We now refer to this activity as AMPylation and the enzyme as an AMPylator. VopS uses this posttranslational modification of AMPylation to hinder signaling between Rho GTPases and their downstream effectors by blocking the effector binding site on the switch I region of the GTPase with AMP.

Both VopS and protein kinases use ATP to modify substrates, but the phosphate attached to the substrate is distinct. Kinases use the γ phosphate of ATP to modify their substrates on tyrosine, threonine and serine residues, whereas VopS uses the α phosphate linked to adenosine to modify its substrate on a threonine residue. This type of modification on eukaryotic proteins is unprecedented. However, it has been observed for a bacterial protein called glutamine synthetase, albeit on a tyrosine residue (*15*). The adenosine 5'-monophosphate modification on glutamine synthetase is autocatalytic, reversible and augments, rather than inhibits, the activity of the modified enzyme (*16*). Because bacterial type III secreted effectors often mimic eukaryotic mechanisms, the observation of AMPylation by a bacterial effector prompted us to investigate whether eukaryotes utilize this posttranslational modification. Incubation of S100 Hela cell lysates with ^{32}P-γ-labeled-ATP predictably reveals many phosphorylated protein substrates (Fig. 4C, lane 5). This modification, phosphorylation, is labile in the presence of a phosphatase (Fig. 4C, lane 8). To test whether the same type of experiment would reveal AMPylated protein substrates, we incubated S100 lysate with ^{32}P-α-labeled ATP. We observe a number of radiolabeled proteins by SDS-PAGE, but in contrast to phosphorylation, these radiolabeled proteins are insensitive to phosphatase treatment (Fig. 4C, lanes 1 and 4, respectively). Addition of purified recombinant VopSΔ30 to the reaction using ^{32}P-α-labeled-ATP, but not ^{32}P-γ-labeled-ATP, specifically increased labeling at the predicted size of the Rho GTPases (Fig. 4C, lanes 2 and 6, respectively). This observation supports the hypothesis that VopS is not a promiscuous AMPylator, but rather targets the Rho family of GTPases. Evidence that AMPylation does not occur spontaneously is seen in Figure 4B where incubation of Rho, Rac, or Cdc42 with ^{32}P-α-

labeled-ATP does not result in a radiolabeled protein. Consistent with this observation, phosphorylation and AMPylation do not occur in the presence of denatured protein (Fig. 4C, lanes 3 and 7, respectively). Based on these observations, we propose that eukarotic proteins use ATP to modify proteins by AMPylation.

A typical bacterial T3SS effector is extremely active, targets a conserved signaling pathway, and mimics/captures a eukaryotic activity (*17*). Herein, we observed that VopS is extremely efficient at inhibiting the activity of Rho GTPases after one hour of infection. In addition, VopS targets the evolutionarily conserved actin cytoskeleton pathway by inactivating Rho GTPases. The modification of proteins with AMP appears to be an activity that is present in eukaryotes and therefore may be a previously undescribed eukaryotic activity that VopS has mimicked or captured.

VopS contains a C-terminal Fic domain, and mutation of an invariant histidine residue within this domain led to the discovery of the catalytic activity of modifying proteins with AMP. We demonstrate that the conserved histidine is critical for the AMPylation activity and that this conserved motif is present in proteins from a diverse set of genomes including bacteria, archaea, metazoa, and a few viruses but absent from most fungi and plants (Fig 1C). The limited eukaryotic distribution of Fic resembles that of other components of signal transduction machinery and might support a role for AMPylation by eukaryotic Fic domains in signaling. Structures of the fic domain solved by the Midwest Center for Structural Genomics and the Joint Center for Structural Genomics place the conserved polar residues of this motif within in a cleft that could represent an active site, with conserved sidechains (from E and N) forming polar contacts with a phosphate in one structure (Fig. S3A). A β-hairpin located near the motif binds peptide in another structure, placing a sidechain of the peptide within Van der Waals contact of the motif Histidine (Fig. S3B). Our studies support the hypothesis that eukaryotes express proteins that use ATP to modify proteins with AMP. This activity represents an ideal posttranslational modification because it: 1) utilizes a highly abundant, high-energy substrate, ATP; 2) results in the formation of a reversible phosphodiester bond; 3) is bulky enough to bind to an adaptor protein and be used in dynamic multidomain signaling complexes; 4) alters the activity of the protein it modifies. It is intriguing that we observe this modification on threonine because this

residue is utilized in many other modifications that might potentially compete with AMPylation. Identification of the substrates and enzymes involved in eukaryotic AMPylation will undoubtedly add a new layer to the expanding complexity of cellular signal transduction (*18*).

Supporting Online Material
www.sciencemag.org

1. N. A. Daniels *et al.*, *J Infect Dis* **181**, 1661 (May, 2000).
2. J. G. Morris, Jr., *Clin Infect Dis* **37**, 272 (Jul 15, 2003).
3. J. B. McLaughlin *et al.*, *N Engl J Med* **353**, 1463 (Oct 6, 2005).
4. K. Makino *et al.*, *Lancet* **361**, 743 (Mar 1, 2003).
5. P. Ghosh, *Microbiol Mol Biol Rev* **68**, 771 (Dec, 2004).
6. K. S. Park *et al.*, *Microbiol Immunol* **48**, 313 (2004).
7. D. L. Burdette, M. L. Yarbrough, A. Orvedahl, C. J. Gilpin, K. Orth, *Proc Natl Acad Sci U S A* **105**, 12497 (Aug 26, 2008).
8. T. Casselli, T. Lynch, C. M. Southward, B. W. Jones, R. DeVinney, *Infect Immun* **76**, 2202 (May, 2008).
9. K. S. Park *et al.*, *Infect Immun* **72**, 6659 (Nov, 2004).
10. A. D. Liverman *et al.*, *Proc Natl Acad Sci U S A* **104**, 17117 (Oct 23, 2007).
11. R. Utsumi, Y. Nakamoto, M. Kawamukai, M. Himeno, T. Komano, *J Bacteriol* **151**, 807 (Aug, 1982).
12. T. Hakoshima, T. Shimizu, R. Maesaki, *J Biochem* **134**, 327 (Sep, 2003).
13. J. B. Bliska, K. L. Guan, J. E. Dixon, S. Falkow, *Proc Natl Acad Sci U S A* **88**, 1187 (Feb 15, 1991).
14. N. Abdul-Manan *et al.*, *Nature* **399**, 379 (May 27, 1999).
15. P. B. Chock, S. G. Rhee, E. R. Stadtman, *Annu Rev Biochem* **49**, 813 (1980).
16. M. S. Brown, A. Segal, E. R. Stadtman, *Proc Natl Acad Sci U S A* **68**, 2949 (Dec, 1971).
17. J. E. Trosky, A. D. Liverman, K. Orth, *Cell Microbiol* **10**, 557 (Mar, 2008).
18. "We thank for insightful discussions and critical reading of the manuscript Neal Alto, Ron Taussig, Paul Sternweis, Sohini Mukherjee, Mike Rosen, Eric Olson, Joe Goldstein, Nick Grishin and Mike Brown. We are extremely grateful to Drs. N. Alto, M. Rosen, P. Sternweis, T. Iida, T. Honda and L. McCarter for their generous supply of reagents. We thank for their generous support and assistance the members of the Orth lab, Amy Haughey and Wanda Simpson. K.O. and M.L.Y. are supported by grants from NIH-AID (R01-AI056404) and the Welch Research Foundation (I-1561). K.O is a Beckman Young Investigator, Burroughs Wellcome Investigator in Infectious Disease, and C.C. Caruth Biomedical Scholar."

Figure Legends

Figure 1. Expression of VopS leads to inactivation of Cdc42 and cell rounding. (**A**) HeLa cells were uninfected (U) or infected with POR3, POR3Δ*vopS (ΔvopS)* or POR3Δ*vopS*+VopS (Δ*vopS+VopS)* over a 4 hour period and tested for active GTP-bound Cdc42 using GST-PAK PBD pulldown assays. Pulldowns and total cell lysates were immunoblotted with anti-Cdc42. As a loading control, total cell lysates were immunoblotted with anti-ß-actin. (**B**) Cells were transfected with pSFFV-eGFP and pcDNA3 empty vector, pcDNA3-VopS, pcDNA3-VopS-H348A, pcDNA3-VopSΔ30 or pcDNA3-VopSΔ30-H348A. Cells were visualized using confocal microscopy for GFP (green) to identify transfected cells and Hoechst to stain nuclei (blue). Scale bar represents 10μm. (**C**) Multiple sequence alignment of representative Fic sequences. Sequences are labeled by species and colored by superkingdom: bacteria (black), eukaryote (blue), archaea (red). Residue positions are highlighted by conservation: hydrophobic (yellow), small (grey), and polar (black). Residue numbers are depicted to the left of the alignment, and omitted residues are in parentheses. Observed secondary structure elements consistent in all Fic domain structures are indicated below the alignment (SS: cylinder for helix and arrow for strand) and colored from N to C-terminus in rainbow. An asterisk above the alignment marks the VopS H348 mutation. Alignments refer to the following proteins in the order listed: VopS, gi|88192876, gi|151567990, gi|42794620, gi|17544594, gi|24582217, and gi|21228708

Figure 2. VopS inhibits *in vitro* binding of the Rho GTPase Rac to its downstream effector PAK. (**A)** GST-pulldown of *in vitro* translated ^{35}S-radiolabeled Rac and GTP-γ-S-loaded ^{35}S-radiolabeled Rac with GST (G), GST-PAK PBD (P), GST-VopSΔ30 (S), or GST-VopSΔ30-H348A (H/A). (**B**) ^{35}S-radiolabeled DA-Rac was pre-incubated with 25 pmoles of VopSΔ30 or VopSΔ30-H348A followed by a pulldown assay with GST-PAK-PBD. (**C**) ^{35}S-radiolabeled DA-Rac was incubated with decreasing concentrations of VopSΔ30 or VopSΔ30-H348A (125 -0.125 pmoles) followed by a pulldown assay with GST-PAK-PBD or GST alone (G). As a positive control, ^{35}S-radiolabeled DA-Rac was

left untreated and pulled down with GST-PAK PBD (U). (**D**) ^{35}S-radiolabeled DA-Rac was incubated over time with 0.25 pmoles of VopSΔ30 or VopSΔ30-H348A followed by pulldown assay with GST-PAK-PBD. Samples were separated by SDS-PAGE and analyzed by autoradiography. All inputs (I) correspond to 5% of material in pulldown.

Figure 3. DA-Rac-VopS is AMPylated on threonine 35 in the switch I region. **(A)** ^{35}S-GTPγS loading of DA-Rac and DA-Rac/VopS. Purified proteins were loaded with radiolabeled GTPγS and subjected to a filter binding assay. Samples were done in triplicate and counts were measured for one minute per sample on a scintillation counter. (**B**) Extracted ion chromatogram (XIC) of the wild-type peptide A (m/z 1488.7) and the modified peptide A (m/z 1653.3) for DA-Rac. The XIC indicates the intensity of the ion as a function of time during the LC/MS/MS process. (**C**) XIC of the wild-type peptide A (m/z 1488.7) and the modified peptide A (m/z 1653.3) for DA-Rac/VopS. (**D**). Electrospray ionization (ESI) tandem mass spectrometry (MS/MS) spectra of modified peptide A. The b and y ions are marked on the MS/MS spectra. Ions corresponded to products of internal fragmentation are marked in brackets. Compared to the MS/MS of the wild-type peptide A (see supplemental data), two forms of mass shift were detected, either with a mass decrease of 18 Da or with a mass increase of 329 Da. Ions with a mass shift are marked with an asterisk. The mass shift started with y3, which indicates that the modification site is Thr35. A further cut of peptide A with AspN resulted in an ion corresponding to peptide B (aa 32-37) with a mass increase of 329 Da (see Fig. S2D). The MS/MS spectrum of the modified peptide B further confirmed that Thr35 is the modification site. (**E**) Alignment of the effector loop region of RhoA, Rac1, and Cdc42. Alignment corresponds to residues 32-50 of RhoA and 30-48 of RacI and Cdc42. Conserved residues are highlighted in red and the switch I region is underlined. The asterisk denotes the AMPylated Thr residue.

Figure 4. *In vitro* AMPylation of Rho family GTPases by VopS. (**A**) Recombinant VopSΔ30 and VopSΔ30-H348A were incubated with or without DA-Rac or DA-Rac-T35A in the presence of ^{32}P-α-labeled ATP. (**B**) Recombinant VopSΔ30 or VopSΔ30-H348A were incubated with GTP-Rho, GTP-Rac or GTP-Cdc42 in the presence of ^{32}P-α-

labeled ATP. (**C**) S100 HeLa cell lysates or boiled, denatured S100 HeLa cell lysates were incubated with ^{32}P-α-labeled ATP or ^{32}P-γ-labeled ATP in the presence or absence of VopSΔ30 (125 pmoles). Samples in lane 4 and 8 were treated with λ-phosphatase (λ-PPase; 400 units) in the last 5 minutes of incubation. Samples were separated by SDS-PAGE and analyzed by autoradiography.

Fig. 1

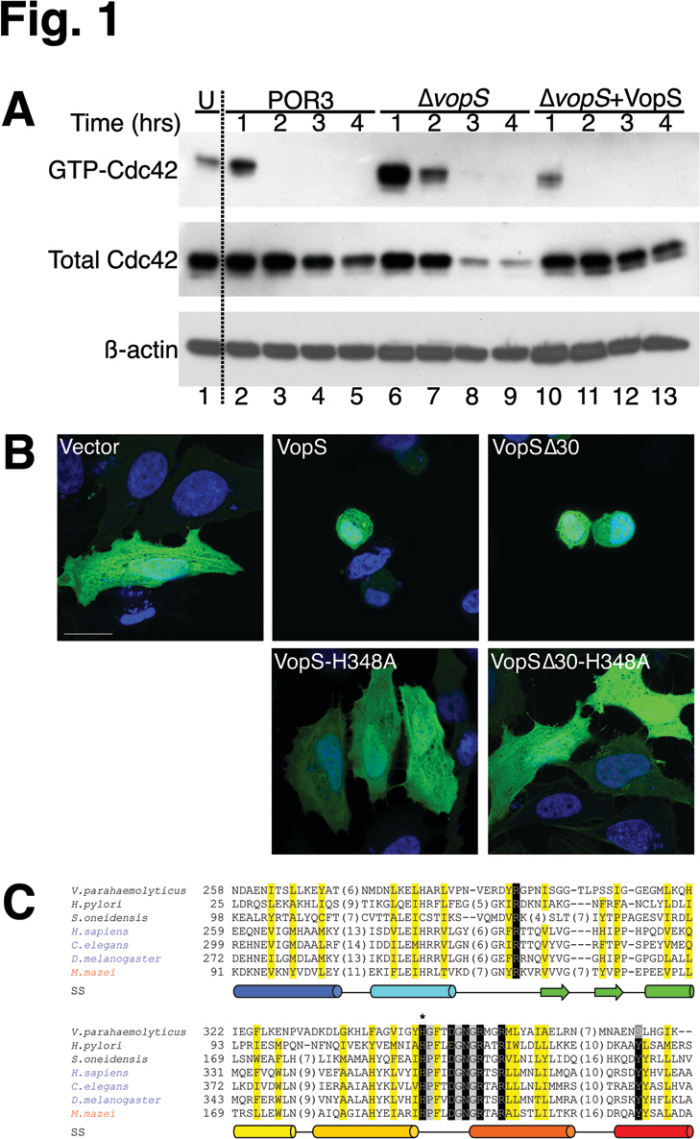
A
U
POR3
ΔvopS
ΔvopS+VopS
Time (hrs)
1 2 3 4 1 2 3 4 1 2 3 4
GTP-Cdc42
Total Cdc42
ß-actin
1 2 3 4 5 6 7 8 9 10 11 12 13
B
Vector
VopS
VopSΔ30
VopS-H348A
VopSΔ30-H348A
C
V.parahaemolyticus 258 NDAENITSLLKEYAT(6)NMDNLKELHARLVPN-VERDYLGPNISGG-TLPSSIG-GEGMLKQH
H.pylori 25 LDRQSLEKAKHLIQS(9)TIKGLQEIHRFLFEG(5)GKIEDKNIAKG---NFRFA-NCLYLDLI
S.oneidensis 98 KEALRYRTALYQCFT(7)CVTTALEICSTIKS--VQMDVEK(4)SLT(7)IYTPPAGESVIRDL
H.sapiens 259 EEQNEVIGMHAAMKY(13)ISDVLEIHRRVLGY(6)GRFITTQVLVG---HHIPP-HPQDVEKQ
C.elegans 299 REHNEVIGMDAALRF(14)IDDILEMHRRVLGN(6)GRITTQVYVG---RFTPV-SPEYVMEQ
D.melanogaster 272 DEHNEILGMDLAMKY(13)IKDILELHRRVLGH(6)GEFIRNQVYVG---GHIPP-GPGDLALL
M.mazei 91 KDKNEVKNYVDVLEY(11)EKIFLEIHRLTVKD(7)GNVEKVRVVVG(7)TVFP-EPEEVPLL
SS
V.parahaemolyticus 322 IEGFLKENPVADKDLGKHLFAGVIGYTGFTDVNDRGMLYAIAELRN(7)MNAENNLHGFK--
H.pylori 93 LPRIESMPQN-NFNQIVEKYVEMNIAPFLDVNDRATGIWLDLLLKKE(10)DKAALSAMERS
S.oneidensis 169 LSNWEAFLH(7)LIKMAMAHYQFEAIPFLDVNDRTGQVLNILYLIDQ(16)HKQDVYRLLLNV
H.sapiens 331 MQEFVQWLN(9)VEFAALAHYKLVYIPFLDVNDRTSKLLMNLILMQA(10)QRSDVYHVLEAA
C.elegans 372 LKDIVDWLN(9)IERAAIAHYKLVLVPFLDVNDRTAGLLLNLLMMRS(10)TRADVYASLHVA
D.melanogaster 343 MQRFERWLN(9)VNYAALAHYKLVHIPFLDVNDRTSKLLMNTLLMRA(10)QRSKDYHFLKLA
M.mazei 169 TRSLLEWLN(9)AIQAGIAHYEIARIPFLDVNDRTAGALSTLILTKR(16)DRQAVYSALADA
SS

Fig. 2

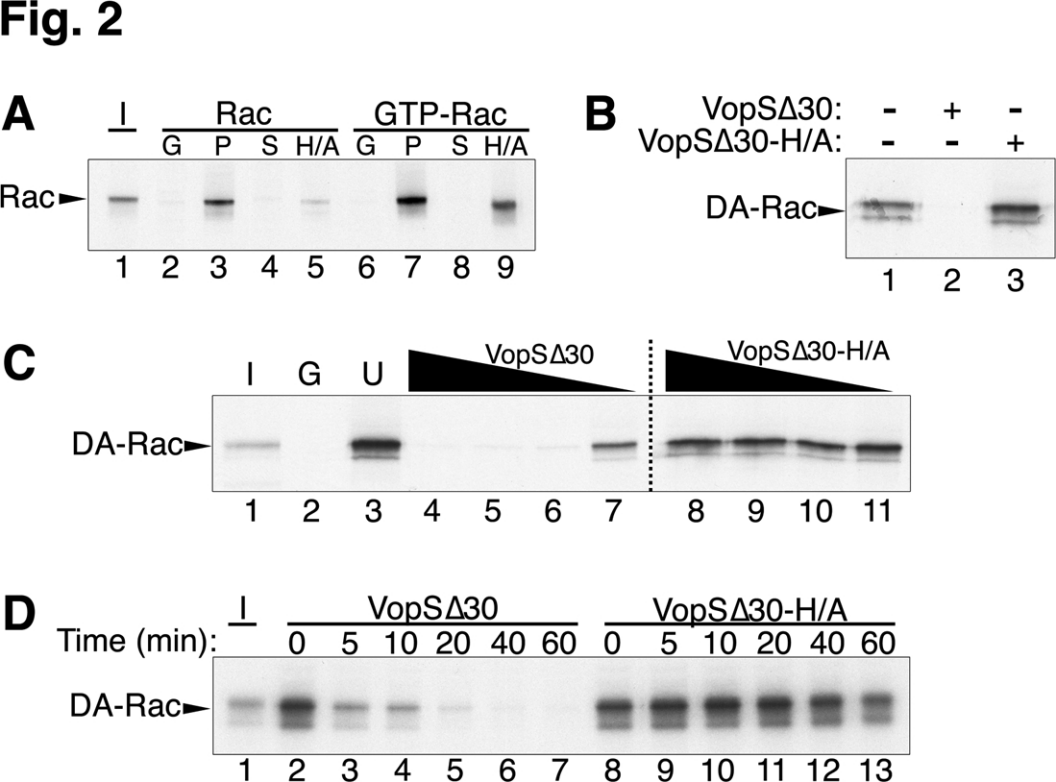
A
I
Rac
GTP-Rac
G P S H/A G P S H/A
Rac
1 2 3 4 5 6 7 8 9
B
VopSΔ30: - + -
VopSΔ30-H/A: - - +
DA-Rac
1 2 3
C
I G U
VopSΔ30
VopSΔ30-H/A
DA-Rac
1 2 3 4 5 6 7 8 9 10 11
D
I
VopSΔ30
VopSΔ30-H/A
Time (min): 0 5 10 20 40 60 0 5 10 20 40 60
DA-Rac
1 2 3 4 5 6 7 8 9 10 11 12 13

Fig. 3

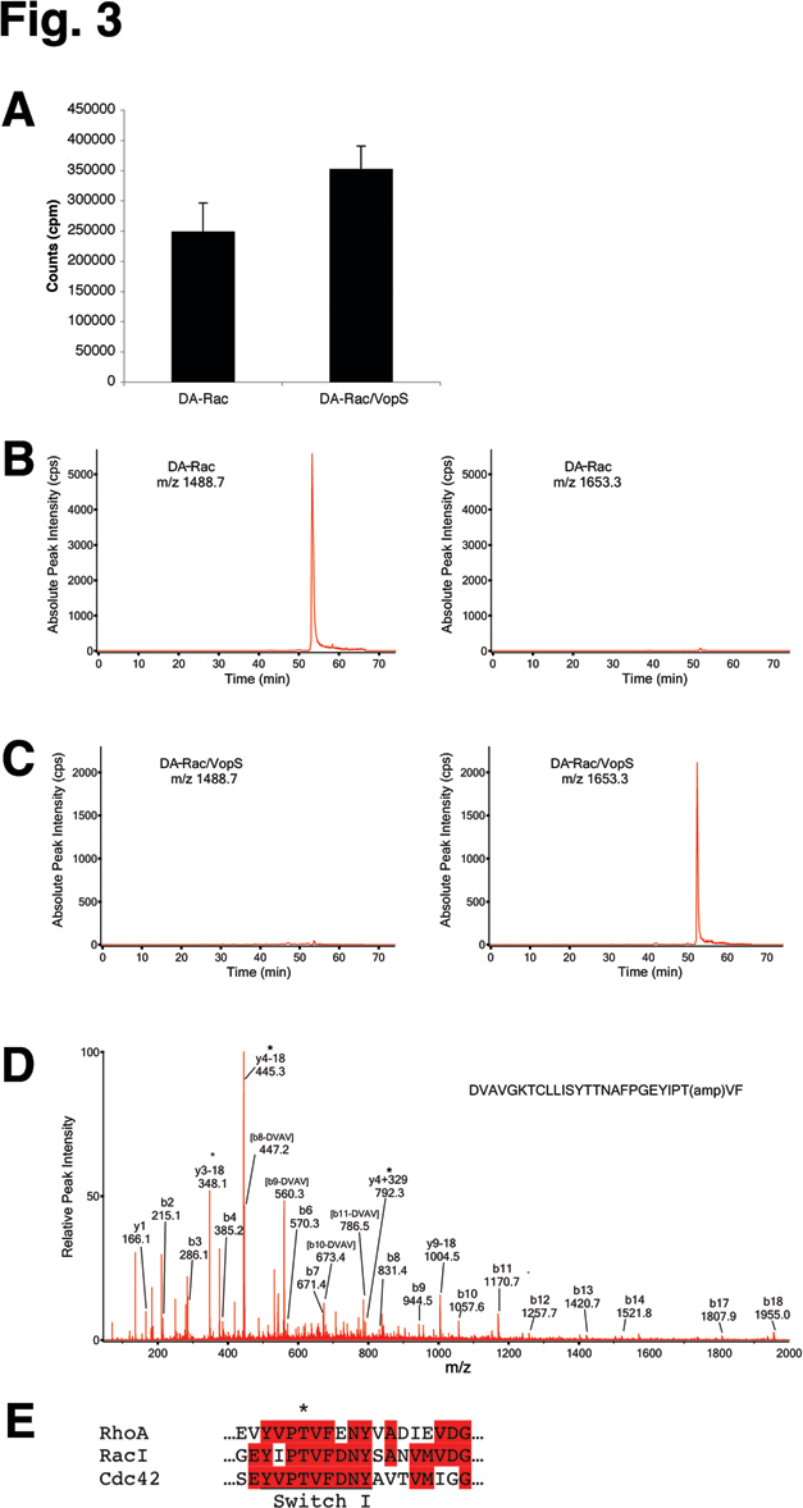
A
Counts (cpm)
450000
400000
350000
300000
250000
200000
150000
100000
50000
0
DA-Rac
DA-Rac/VopS
B
DA-Rac
m/z 1488.7
Absolute Peak Intensity (cps)
Time (min)
DA-Rac
m/z 1653.3
C
DA-Rac/VopS
m/z 1488.7
DA-Rac/VopS
m/z 1653.3
D
Relative Peak Intensity
m/z
DVAVGKTCLLISYTTNAFPGEYIPT(amp)VF
y4-18
445.3
y3-18
348.1
[b8-DVAV]
447.2
[b9-DVAV]
560.3
y4+329
792.3
[b11-DVAV]
786.5
[b10-DVAV]
673.4
y1
166.1
b2
215.1
b3
286.1
b4
385.2
b6
570.3
b7
671.4
b8
831.4
b9
944.5
y9-18
1004.5
b10
1057.6
b11
1170.7
b12
1257.7
b13
1420.7
b14
1521.8
b17
1807.9
b18
1955.0
E
RhoA ...EVYVPTVFENYVADIEVDG...
RacI ...GEYIPTVFDNYSANVMVDG...
Cdc42 ...SEYVPTVFDNYAVTVMIGG...
Switch I

Fig. 4

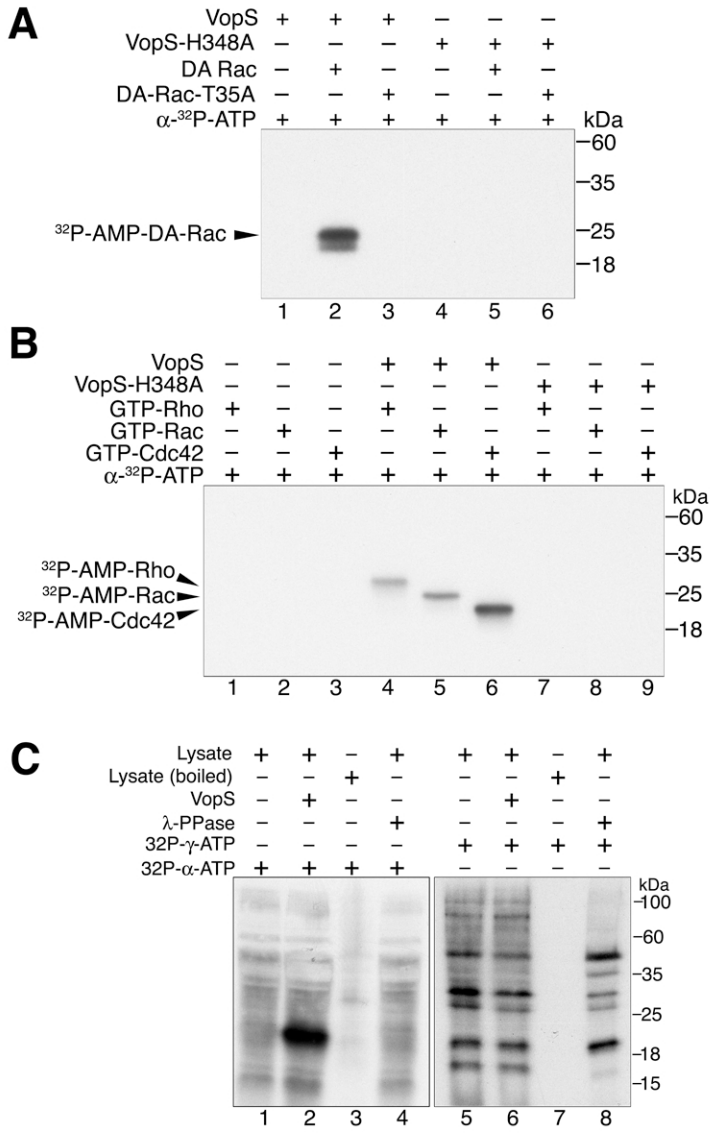
A
VopS + + + – – –
VopS-H348A – – – + + +
DA Rac – + – – + –
DA-Rac-T35A – – + – – +
α-32P-ATP + + + + + +
kDa
60
35
25
18
32P-AMP-DA-Rac
1 2 3 4 5 6
B
VopS – – – + + + – – –
VopS-H348A – – – – – – + + +
GTP-Rho + – – + – – + – –
GTP-Rac – + – – + – – + –
GTP-Cdc42 – – + – – + – – +
α-32P-ATP + + + + + + + + +
kDa
60
35
25
18
32P-AMP-Rho
32P-AMP-Rac
32P-AMP-Cdc42
1 2 3 4 5 6 7 8 9
C
Lysate + + – + + + – +
Lysate (boiled) – – + – – – + –
VopS – + – – – + – –
λ-PPase – – – + – – – +
32P-γ-ATP – – – – + + + +
32P-α-ATP + + + + – – – –
kDa
100
60
35
25
18
15
1 2 3 4 5 6 7 8